

Strain-induced stripe phase in charge ordered single layer NbSe₂

Fabrizio Cossu,^{1,*} Igor Di Marco,^{1,2,3} and Alireza Akbari^{1,3,4,†}

¹*Asia Pacific Center for Theoretical Physics, Pohang, 37673, Korea*

²*Department of Physics and Astronomy, Uppsala University, Box 516, SE-75120, Uppsala, Sweden*

³*Department of Physics, POSTECH, Pohang, 37673, Korea*

⁴*Max Planck POSTECH Center for Complex Phase Materials, POSTECH, Pohang 790-784, Korea*

(Dated: January 27, 2023)

Charge density waves are ubiquitous phenomena in metallic transition metal dichalcogenides. In NbSe₂, a trigonal 3×3 structural modulation is coupled to a charge modulation. Recent experiments reported that a trigonal-stripe transition occurred at the surface, possibly due to local strain and/or accidental doping. We employ *ab-initio* calculations to investigate the structural instabilities arising from strain in a pristine single layer and analyze the energy hierarchy of the structural and charge modulations. Our *ab-initio* calculations support the observation of phase separation between trigonal and stripe phases in NbSe₂ single layers and surface in the clean limit, reproducing it with the observed wavelength.

Transition metal dichalcogenides are among the most exciting hosts for ordered phases, such as superconductivity and charge/spin modulations [1–5], showing strong evidences for cooperative interaction between them [6]. The coexistence of these phases is counter-intuitive, considering they are collective electronic modes which build an excitation gap, hence requiring a large number of electrons available at Fermi level. Since early works [7–9], the transition to a charge/spin ordered state driven by the electron gas at Fermi level was questioned, also on the basis of an intricate coexistence of superconductivity with charge density waves (CDWs) [2, 4, 5, 10–12]; recently, the electronically driven mechanism was ruled out [13–19] in favor of a momentum-assisted mechanism [8, 10, 18, 20–22, 24], which is likely influenced by external conditions, such as applied fields [12, 25] or epitaxially induced strain [26, 27], and chemical [7, 28, 29] or gate [27, 31] doping.

Further intricacies arise from the occurrence of these phenomena at the surface or single layers, which may be accompanied by dramatic changes in structural and electronic degrees of freedom [32–38]. Lack of inversion symmetry and van der Waals bonded layers may result in remarkably different behavior with respect to the bulk [39–41]. The 2H-1T crystal phase transition at the surface of NbSe₂ [42, 43] (the 1T crystal phase is unstable in the bulk [44]), the occurrence of 4×4 [3, 4] and/or a 2×2 [4] modulations, linked to a stripe phase, and the observation of distinct charge density wave structures, determining a factor for the incommensuration character [6], are just a few recent examples. A change from the 3×3 to the 4×4 modulation was previously predicted by *ab-initio* studies [20, 48]; on the other hand, a recent study [5] showed that within a 3×3 modulation, uniaxial strain leads to a trigonal-stripe CDW transition. However, phase transitions remain often latent because

they are suppressed by growing/synthesis conditions or quantum fluctuations. In this respect, discerning intrinsic from extrinsic characteristics is crucial to understand these phases and finding possible routes to their manipulation.

In order to shed light into the competition and coexistence of various periodicities and structures, we present a study based on phonon calculations and a full set of total energy calculations of single layer NbSe₂ without defects. We establish an energy hierarchy for a large range of structures and we find a connection with the $3\mathbf{q}\cdot\mathbf{1q}$ (triangular-stripe) transition. The present manuscript investigates such transition, showing that it is incipient (occurs) in the 3×3 (4×4) modulation.

Our results are obtained by *ab initio* calculations within the formalism of the density-functional theory (DFT). The projected augmented wave (PAW) method with Perdew-Burke-Ernzerhof (PBE) pseudopotentials [50, 51], as implemented in the QUANTUM ESPRESSO suite [52, 53] and the Vienna Ab-initio Simulation Package (VASP), is used. The relaxation of the unit cell and the computation of its relative phononic spectra are run in the former code, while structural relaxation, total energy calculations and charge distributions are performed with the latter. Further computational details are given in the supplemental information.

Structural relaxation of the unit cell yields an in-plane stress of $7.9 \times 10^{-5} \text{ Ry/Bohr}^3$, $1.2 \times 10^{-5} \text{ Ry/Bohr}^3$, and $-4.9 \times 10^{-5} \text{ Ry/Bohr}^3$ with the lattice constants of 3.41 Å, 3.45 Å, and 3.49 Å, respectively. The phonon dispersion is computed for these three values of the in-plane lattice constant and plotted as two-dimensional densities in FIG. 1. Negative values of $(\omega(\mathbf{q}))^2$ are represented in red. Our analysis considers lattice reconstructions of the type $\sqrt{n} \times \sqrt{n}$, in line with ref. 54, and $n \times m$, suggested by scanning tunnelling microscopy [6] results.

The deepest trough signalling the instability (the lowest value of $(\omega(\mathbf{q}))^2$) is found off the ΓM line for no strain, in a region towards the $\sqrt{13} \times \sqrt{13}$ modulation, for the single layer, whereas the bulk features instabilities dominating along ΓM , in agreement with the 3×3

* nome.cognome@europe.com

† alireza@apctp.org

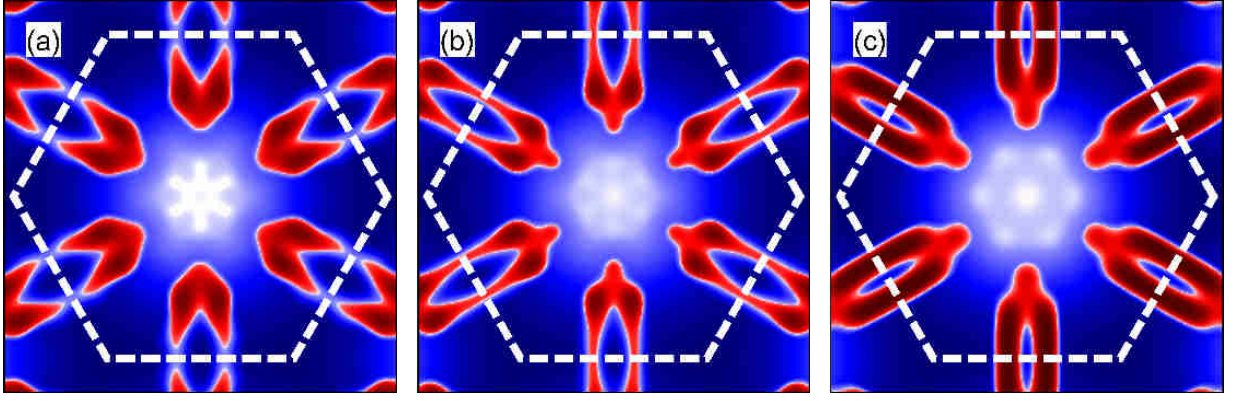


FIG. 1. (Colour online) Two-dimensional phonon dispersion for the NbSe₂ single layer unit cell as two-dimensional density plots, under compressive strain (a), at the equilibrium lattice constant (b), and under tensile strain (c). The plots, as function of k_x and k_y , in units of $2\pi/a$, show only the branch with the lowest values of $\omega^2(\mathbf{q})$; red (blue) represent regions of negative (positive) values of $\omega^2(\mathbf{q})$.

periodicity [20], see FIG. S1. The sharp minima in the phonon dispersion of the single layer, located near the $\sqrt{13} \times \sqrt{13}$ region, support a recently observed 2H-1T structural transition [42, 43].

Compressive strain reduces instabilities along the MK line and the minima of $(\omega(\mathbf{q}))^2$ dominate around 2/4 ΓM (off the high symmetry line), FIG. 1. Conversely, a zone of instability centered around, but not including, M becomes dominant under tensile strain, and further local minima of $(\omega(\mathbf{q}))^2$ appear at 2/4 ΓM , supporting recent reports [4] for which both 2×2 and 4×4 periodicities arise under tensile strain.

We now explore the CDW formation by total energy calculations in different supercells. Each one has a periodicity which is the smallest possible in agreement with the calculated phonon spectra; in addition, we refer to experimental findings [4, 6]. We study a representative number of structures for each periodicity (in the 3×3 periodicity we study three known CDW structures [6, 7, 48, 55] anew, complementing previous studies with the trend of the energy hierarchy upon strain); here we refer to them as hexagonal (HX), chalcogen centered triangular (CC), and hollow centered triangular (HC). Total energy calculations are used to test whether and how each periodicity can give rise to a CDW structure.

Supercell calculations show that all 2×2 structures relaxed to the symmetric structure with the same energy for all values of the strain; therefore, no 2×2 periodicity is expected for a free-standing single layer. Structures related to the 2×3 periodicity are instead found to relax to a stripe phase (different structures converge to a unique phase), see FIG. S2, which also illustrates how HC and CC can merge. The existence of such periodicity represents a solid explanation for the boundary between HC and CC CDW structures observed via STM [6] in regions where the two coexist. Three structures are found with the $\sqrt{13} \times \sqrt{13}$ and with the 4×4 periodicity, all competing with the 3×3 CDWs, and they are illustrated in FIG. S3, supplemental information. In particular, the

ones in the 4×4 supercell are favored with respect to the well known 3×3 modulations under compressive strain. In general, phononic calculations support the idea that a plethora of structural modulations is available in single layer NbSe₂, which compete under certain circumstances (such as epitaxial strain, charge transfer or proximity effects). Total energy results are summarized in TABLE I.

Three structures with the 4×4 periodicity exist at the equilibrium lattice constant, two of them characterized by a single ordering vector ($1\mathbf{q}'$ and $1\mathbf{q}''$), favored with respect to a third one, characterized by three equivalent ordering vectors ($3\mathbf{q}$); the latter also degenerates into the $1\mathbf{q}'$ ($1\mathbf{q}''$) for compressive (tensile) strain, see FIG. 2. A remarkable agreement between the measured [3] and calculated wavelength of the modulation ($\sim 12\text{\AA}$ and 11.8\AA , respectively) and the FT of the resulting charge distribution (FIG. S4 in the supplemental information with figure 1F in ref. [4]) suggests with a considerable level of confidence that this phase(s) are those connected to the observed stripe phase, see FIG. 2.

Further consideration is deserved by the mixing of the ‘elemental’ 3×3 CDW structures in the 4×4 CDW structures, apparent in FIG. 2 and similar to the mixing of 3×3 CDW structures, as illustrated in FIG. S2, supplemental information. Such observations suggest an intricate relation between different phases, where strain plays a paramount role. While we can imagine an average strain applied to the single layer by a substrate, different phases may be favored by slight variations of strain, as shown from TABLE I; as a consequence, separated regions may host different CDW phases [6] connected by a boundary. The present manuscript supports this idea, giving it solid grounds in terms of total energy calculations and structural analysis, pointing to a 2×3 modulation as the boundary between the 3×3 -modulated HC and CC CDW phases.

The isotropic nature of the simulated strain in the work presented here (as opposed to a work on uniaxial

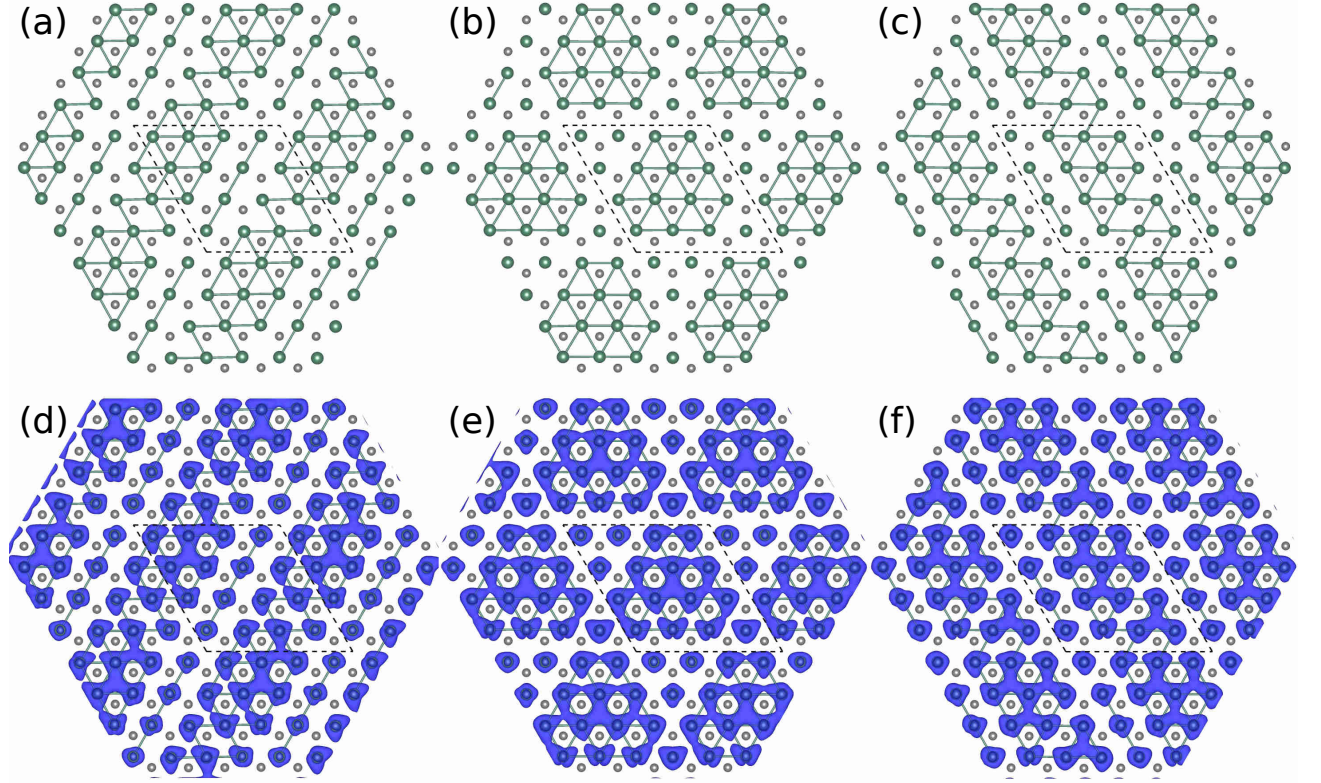


FIG. 2. Structures (a-c) and corresponding charge (d-f) modulations resulting from a 4×4 periodicity. In the stripe phases $1\mathbf{q}'$ (d) and $1\mathbf{q}''$ (f), the wavelengths is 11.8 Å. Dark green (grey) spheres represent Nb (Se) atoms; Nb-Nb bonds shorter than the equilibrium distance (the respective lattice constant) are represented by solid lines, in order to help visualising the CDW structure pattern. Dashed lines mark the supercells borders.

TABLE I. Total energy difference with respect to the fully symmetric structure of various structures, grouped per periodicity, at three different values of the in-plane lattice constant. The energy for each structure is the difference, expressed in meV/f.u., with the energy of the symmetric structure, and it is negative for favored structures. The three structures with $\sqrt{13} \times \sqrt{13}$ periodicity are illustrated in the supplemental information.

	2×3		3×3			$\sqrt{13} \times \sqrt{13}$			4×4		
	MM	MW	HX	CC	HC	CCcws	HXHC	HC	$1\mathbf{q}'$	$3\mathbf{q}$	$1\mathbf{q}''$
$ \mathbf{a} = 3.49$	-1.9	-0.9	-3.0	-3.5	-4.4	-0.3	-0.4	-0.4	-6.2	-4.3	-2.8
$ \mathbf{a} = 3.45$	-1.9	-0.0	-2.8	-3.4	-4.0	-1.4	-0.6	-1.4	-4.4	-2.5	-4.3
$ \mathbf{a} = 3.41$	-2.3	-0.0	-2.8	-3.6	-3.6	-3.4	-2.4	-3.6	-6.2	-6.2	-6.2

strain [5]), raises interesting points of discussion, such as the behavior of the electron-phonon coupling in NbSe₂ and the competition of various order parameters in the CDW phase. In the work by Flicker and van Wezel [5], phonon fluctuations suppress long-range order in favor of a short-ranged pseudogap phase with a $3\mathbf{q}$ phase, which degenerates into a $1\mathbf{q}$ phase upon uniaxial strain. Our finding show that isotropic strain is sufficient to reduce the symmetry of the charge distribution (hence, of the ordering parameters space), if a different periodicity (4×4 , supported by phonon and total energy calculations) is assumed. On the other hand, isotropic strain in a 3×3 periodicity induces only an incipient stripe phase with a 3×3 periodicity, see FIG. S5 in the supplemental information.

The modulation itself, and not merely the strain, determines the relation between the order parameters, because the electron-phonon interaction and the periodic lattice modulation are strictly related [56]. Moreover, FIG. S5 in the supplemental information, shows how the ground state CDW of the 3×3 modulation behaves under strain. The HC and CC CDW structures are distinct under tensile strain and at the equilibrium lattice constant, but the HC degenerates into the CC for compressive strain, reinforcing the hypothesis that the boundary between these two CDWs are accompanied by the formation of a CDW with 2×3 periodicity.

With reference to FIG. 3, we compare the density of the electronic states (DOS) of the single-vector CDWs

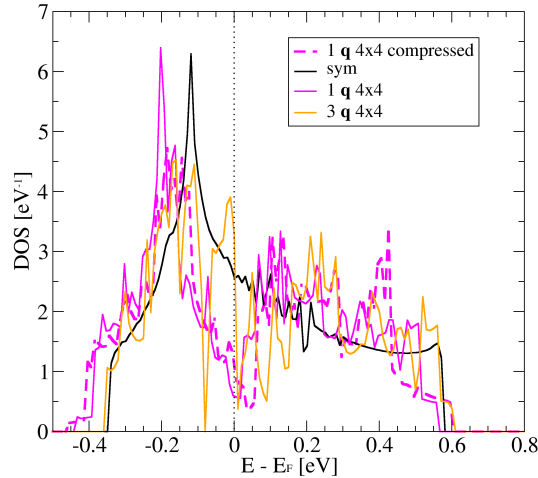


FIG. 3. Density of the electronic states (DOS) of the non modulated structure (in black) and two representative CDW structures with a 4×4 periodicity, $1\mathbf{q}'$ and $3\mathbf{q}$ (DOS curves for CDW structures with a single ordering vector do not differ sensibly). The value of the DOS is rescaled for one unit cell, for a meaningful comparison between DOS curves of different supercells.

(denoted both as $1\mathbf{q}$ because their DOS curves have no substantial difference) and the $3\mathbf{q}$ CDW structures. The $3\mathbf{q}$ CDW features a DOS with a clear and narrow dip at ~ -0.08 eV and an enhancement of the spectral weight at Fermi level, whereas the $1\mathbf{q}$ CDW features a depletion of spectral weight around Fermi level. Accordingly, a CDW phase change, as resolved in direct space [8] of the $3\mathbf{q}$ CDW is observed, see FIG. S6 in the supplemental information. The symmetry of the $3\mathbf{q}$ CDW becomes disper-

sive below the Nb band, at the bottom of which a stripe character is observed. This confirms that the character of the interaction responsible for such CDW is moderately correlated, in line with previous studies [10]. Finally, the enhancement of states at Fermi level suggests an enhanced transition temperature for the superconducting phase from the $3\mathbf{q}$ CDW - compare its spectral weight with that of other CDWs [7, 48]. However, the DOS curve of the $1\mathbf{q}$ CDW is in stronger agreement with experimental data [34], featuring a depletion of states at Fermi level.

In conclusion, we demonstrated that the stripe phase in single layer NbSe₂ is associated to a 4×4 modulation, highly favored by compressive, isotropic strain; moreover, we investigate the connection between triple and single ordering vectors geometries in the 4×4 modulation. Conversely, the 3×3 periodicity allows only an incipient $3\mathbf{q}$ - $1\mathbf{q}$ transition under strain, but an interesting connection is found between the ground state CDW structures, reporting their structural character and energy competition.

We are grateful to Yunkyu Bang, Erio Tosatti, Stefano de Gironcoli, Ali G. Moghaddam, Tristan Cren, Hermann Suderow, and Han-Woong Yeom for insightful discussions. F. C. and A. A. acknowledge financial support from the National Research Foundation (NRF) funded by the Ministry of Science of Korea (Grants No. 2017R1D1A1B03033465, & No. 2019R1H1A2039733). This research was supported by appointments to the JRG program at the APCTP through the Science and Technology Promotion Fund and Lottery Fund of the Korean Government. It also received support by the Korean Local Governments - Gyeongsangbuk-do Proving and Pohang City.

-
- [1] Y. Saito, T. Nojima, and Y. Iwasa, *Nature Reviews Materials* **2**, 16094 EP (2016).
 - [2] J. A. Wilson, F. J. Di Salvo, and S. Mahajan, *Phys. Rev. Lett.* **32**, 882 (1974).
 - [3] J. A. Wilson, F. J. D. Salvo, and S. Mahajan, *Advances in Physics* **50**, 1171 (2001).
 - [4] D. E. Moncton, J. D. Axe, and F. J. DiSalvo, *Phys. Rev. Lett.* **34**, 734 (1975).
 - [5] E. Revolinsky, G. A. Spiering, and B. D. J., *J. Phys. Chem. Solids* **26**, 1029 (1965).
 - [6] T. Kiss, T. Yokoya, A. Chainani, S. Shin, T. Hanaguri, M. Nohara, and H. Takagi, *Nat. Phys.* **3**, 720 EP (2007), article.
 - [7] T. M. Rice and G. K. Scott, *Phys. Rev. Lett.* **35**, 120 (1975).
 - [8] R. Liu, C. G. Olson, W. C. Tonjes, and R. F. Frindt, *Phys. Rev. Lett.* **80**, 5762 (1998).
 - [9] T. Straub, T. Finteis, R. Claessen, P. Steiner, S. Hüfner, P. Blaha, C. S. Oglesby, and E. Bucher, *Phys. Rev. Lett.* **82**, 4504 (1999).
 - [10] D. J. Rahn, S. Hellmann, M. Kalläne, C. Sohrt, T. K. Kim, L. Kipp, and K. Rossnagel, *Phys. Rev. B* **85**, 224532 (2012).
 - [11] A. H. Castro Neto, *Phys. Rev. Lett.* **86**, 4382 (2001).
 - [12] K. Cho, M. Konczykowski, S. Teknowijoyo, M. A. Tanatar, J. Guss, P. B. Gartin, J. M. Wilde, A. Kreyssig, R. J. McQueeney, A. I. Goldman, V. Mishra, P. J. Hirschfeld, and R. Prozorov, *Nat. Commun.* **9**, 2796 (2018).
 - [13] D. S. Inosov, V. B. Zabolotnyy, D. V. Evtushinsky, A. A. Kordyuk, B. Büchner, R. Follath, H. Berger, and S. V. Borisenko, *New J. Phys.* **10**, 125027 (2008).
 - [14] K. Rossnagel, O. Seifarth, L. Kipp, M. Skibowski, D. Voß, P. Krüger, A. Mazur, and J. Pollmann, *Phys. Rev. B* **64**, 235119 (2001).
 - [15] K. Rossnagel and N. V. Smith, *Phys. Rev. B* **76**, 073102 (2007).
 - [16] M. D. Johannes, I. I. Mazin, and C. A. Howells, *Phys. Rev. B* **73**, 205102 (2006).
 - [17] M. D. Johannes and I. I. Mazin, *Phys. Rev. B* **77**, 165135 (2008).
 - [18] X. Zhu, Y. Cao, J. Zhang, E. W. Plummer, and J. Guo,

- Proc. Natl. Acad. Sci. **112**, 2367 (2015).
- [19] J. Ángel Silva-Guillén, P. Ordejón, F. Guinea, and E. Canadell, *2D Materials* **3**, 035028 (2016).
- [20] M. Calandra, I. I. Mazin, and F. Mauri, *Phys. Rev. B* **80**, 241108 (2009).
- [21] T. Valla, A. V. Fedorov, P. D. Johnson, P.-A. Glans, C. McGuinness, K. E. Smith, E. Y. Andrei, and H. Berger, *Phys. Rev. Lett.* **92**, 086401 (2004).
- [22] F. Zheng, Z. Zhou, X. Liu, and J. Feng, *Phys. Rev. B* **97**, 081101 (2018).
- [8] C. J. Arguello, S. P. Chockalingam, E. P. Rosenthal, L. Zhao, C. Gutiérrez, J. H. Kang, W. C. Chung, R. M. Fernandes, S. Jia, A. J. Millis, R. J. Cava, and A. N. Pasupathy, *Phys. Rev. B* **89**, 235115 (2014).
- [24] F. Flicker and J. van Wezel, *Nat. Commun.* **6**, 7034 EP (2015), article.
- [25] J. A. Galvis, E. Herrera, C. Berthod, S. Vieira, I. Guilmón, and H. Suderow, *Communications Physics* **1**, 30 (2018).
- [26] Z.-G. Fu, J.-H. Wang, Y. Yang, W. Yang, L.-L. Liu, Z.-Y. Hu, and P. Zhang, *EPL (Europhysics Letters)* **120**, 17006 (2017).
- [27] M. J. Wei, W. J. Lu, R. C. Xiao, H. Y. Lv, P. Tong, W. H. Song, and Y. P. Sun, *Phys. Rev. B* **96**, 165404 (2017).
- [28] F. J. Di Salvo, J. A. Wilson, B. G. Bagley, and J. V. Waszczak, *Phys. Rev. B* **12**, 2220 (1975).
- [29] U. Chatterjee, J. Zhao, M. Iavarone, R. Di Capua, J. P. Castellán, G. Karapetrov, C. D. Malliakas, M. G. Kanatzidis, H. Claus, J. P. C. Ruff, F. Weber, J. van Wezel, J. C. Campuzano, R. Osborn, M. Randeria, N. Trivedi, M. R. Norman, and S. Rosenkranz, *Nat. Commun.* **6**, 6313 EP (2015).
- [7] F. Cossu, A. G. Moghaddam, K. Kim, H. A. Tahini, I. Di Marco, H.-W. Yeom, and A. Akbari, *Phys. Rev. B* **98**, 195419 (2018).
- [31] D. F. Shao, R. C. Xiao, W. J. Lu, H. Y. Lv, J. Y. Li, X. B. Zhu, and Y. P. Sun, *Phys. Rev. B* **94**, 125126 (2016).
- [32] R. F. Frindt, *Phys. Rev. Lett.* **28**, 299 (1972).
- [33] X. Xi, L. Zhao, Z. Wang, H. Berger, L. Forró, J. Shan, and K. F. Mak, *Nat Nano* **10**, 765 (2015).
- [34] M. M. Ugeda, A. J. Bradley, Y. Zhang, S. Onishi, Y. Chen, W. Ruan, C. Ojeda-Aristizabal, H. Ryu, M. T. Edmonds, H.-Z. Tsai, A. Riss, S.-K. Mo, D. Lee, A. Zettl, Z. Hussain, Z.-X. Shen, and M. F. Crommie, *Nat. Phys.* **12**, 92 (2016).
- [35] S. Z. Butler, S. M. Hollen, L. Cao, Y. Cui, J. A. Gupta, H. R. Gutiérrez, T. F. Heinz, S. S. Hong, J. Huang, A. F. Ismach, E. Johnston-Halperin, M. Kuno, V. V. Plashnitsa, R. D. Robinson, R. S. Ruoff, S. Salahuddin, J. Shan, L. Shi, M. G. Spencer, M. Terrones, W. Windl, and J. E. Goldberger, *ACS Nano* **7**, 2898 (2013).
- [36] A. K. Geim and I. V. Grigorieva, *Nature* **499**, 419 (2013).
- [37] K. S. Novoselov, A. Mishchenko, A. Carvalho, and A. H. Castro Neto, *Science* **353**, aac9439 (2016).
- [38] Y. Ge and A. Y. Liu, *Phys. Rev. B* **86**, 104101 (2012).
- [39] V. N. Kotov, B. Uchoa, V. M. Pereira, F. Guinea, and A. H. Castro Neto, *Rev. Mod. Phys.* **84**, 1067 (2012).
- [40] F. Guinea, M. I. Katsnelson, and T. O. Wehling, *Annalen der Physik* **526**, A81 (2014).
- [41] K. F. Mak, K. He, C. Lee, G. H. Lee, J. Hone, T. F. Heinz, and J. Shan, *Nat. Mater.* **12**, 207 EP (2012).
- [42] Y. Nakata, K. Sugawara, R. Shimizu, Y. Okada, P. Han, T. Hitosugi, K. Ueno, T. Sato, and T. Takahashi, *Npg Asia Materials* **8**, e321 EP (2016).
- [43] F. Bischoff, W. Auwärter, J. V. Barth, A. Schiffrin, M. Fuhrer, and B. Weber, *Chemistry of Materials* **29**, 9907 (2017), <https://doi.org/10.1021/acs.chemmater.7b03061>.
- [44] F. Kadijk and F. Jellinek, *Journal of the Less Common Metals* **23**, 437 (1971).
- [3] A. Soumyanarayanan, M. M. Yee, Y. He, J. van Wezel, D. J. Rahn, K. Rossnagel, E. W. Hudson, M. R. Norman, and J. E. Hoffman, *Proc. Natl. Acad. Sci.* **110**, 1623 (2013).
- [4] S. Gao, F. Flicker, R. Sankar, H. Zhao, Z. Ren, B. Rachmilowitz, S. Balachandar, F. Chou, K. S. Burch, Z. Wang, J. van Wezel, and I. Zeljkovic, *Proc. Natl. Acad. Sci.* **115**, 6986 (2018).
- [6] G. Gye, E. Oh, and H. W. Yeom, *Phys. Rev. Lett.* **122**, 016403 (2019).
- [48] C.-S. Lian, C. Si, and W. Duan, *Nano Letters* **18**, 2924 (2018).
- [5] F. Flicker and J. van Wezel, *Phys. Rev. B* **92**, 201103 (2015).
- [50] P. E. Blöchl, *Phys. Rev. B* **50**, 17953 (1994).
- [51] G. Kresse and D. Joubert, *Phys. Rev. B* **59**, 1758 (1999).
- [52] P. Giannozzi, S. Baroni, N. Bonini, M. Calandra, R. Car, C. Cavazzoni, D. Ceresoli, G. L. Chiarotti, M. Cococcioni, I. Dabo, A. D. Corso, S. de Gironcoli, S. Fabris, G. Fratesi, R. Gebauer, U. Gerstmann, C. Gougoussis, A. Kokalj, M. Lazzeri, L. Martin-Samos, N. Marzari, F. Mauri, R. Mazzarello, S. Paolini, A. Pasquarello, L. Paulatto, C. Sbraccia, S. Scandolo, G. Sclauzero, A. P. Seitsonen, A. Smogunov, P. Umari, and R. M. Wentzcovitch, *J. Phys.: Condens. Matter* **21**, 395502 (2009).
- [53] P. Giannozzi, O. Andreussi, T. Brumme, O. Bunau, M. B. Nardelli, M. Calandra, R. Car, C. Cavazzoni, D. Ceresoli, M. Cococcioni, N. Colonna, I. Carnimeo, A. D. Corso, S. de Gironcoli, P. Delugas, R. A. DiStasio, A. Ferretti, A. Floris, G. Fratesi, G. Fugallo, R. Gebauer, U. Gerstmann, F. Giustino, T. Gorni, J. Jia, M. Kawamura, H.-Y. Ko, A. Kokalj, E. Küçükbenli, M. Lazzeri, M. Marsili, N. Marzari, F. Mauri, N. L. Nguyen, H.-V. Nguyen, A. O. de-la Roza, L. Paulatto, S. Poncé, D. Rocca, R. Sabatini, B. Santra, M. Schlipf, A. P. Seitsonen, A. Smogunov, I. Timrov, T. Thonhauser, P. Umari, N. Vast, X. Wu, and S. Baroni, *J. Phys.: Condens. Matter* **29**, 465901 (2017).
- [54] E. Kamil, J. Berges, G. Schönhoff, M. Rösner, M. Schüler, G. Sangiovanni, and T. O. Wehling, *J. Phys.: Condens. Matter* **30**, 325601 (2018).
- [55] C. D. Malliakas and M. G. Kanatzidis, *J. Am. Chem. Soc.* **135**, 1719 (2013).
- [56] F. Weber, S. Rosenkranz, J.-P. Castellán, R. Osborn, R. Hott, R. Heid, K.-P. Bohnen, T. Egami, A. H. Said, and D. Reznik, *Phys. Rev. Lett.* **107**, 107403 (2011).
- [1] J. P. Perdew, K. Burke, and M. Ernzerhof, *Phys. Rev. Lett.* **77**, 3865 (1996).
- [2] J. P. Perdew, K. Burke, and M. Ernzerhof, *Phys. Rev. Lett.* **78**, 1396 (1997).

SUPPLEMENTAL MATERIAL FOR TRIANGULAR-STRIPE TRANSITION IN CHARGE ORDERED SINGLE LAYER NBSE₂ BY

Fabrizio Cossu, Igor Di Marco, and Alireza Akbari

I. METHODS

The study presented here is based on density functional formalism, using two codes with a plane wave basis set both based on the pseudopotential method, the Vienna Ab-initio Simulation Package (VASP) and QUANTUM ESPRESSO. We perform supercells calculations on the former, and single cell calculations using the density functional perturbation theory on the latter (to compute phonon dispersion). The exchange-correlation functional is treated within the generalized gradient approximation using the PBE parametrisation [S1, S2]. The pseudopotentials used in the simulations provide explicit treatment of the following valence electrons for Nb and Se, respectively: $4s^2 4p^6 5s^1 5d^4$ and $4s^2 4p^4$. The cutoff energy of the plane waves for the unit cell (QUANTUM ESPRESSO) is ~ 1142 eV and that for the supercell calculations is 500 eV; prior to the phonon calculations, an energy cutoff is also applied for the charge density and potential, of ~ 4354 eV (these numbers are converted from Ry, the energy unit used by QUANTUM ESPRESSO). The energy tolerance on the electronic loops for the calculations in the unit cell is $1.4 \cdot 10^{-9}$ eV, whereas it is 10^{-6} eV for the calculations in the supercells (10^{-7} eV for the accurate determination of the electronic properties, such as density of electronic states and charge distributions). A conjugate gradient algorithm is employed for structural relaxation in all cases with a tolerance of 10^{-3} eV/Å⁻¹ for the unit cell, and 10^{-4} eV per unit cell (in energy, with a residual force of ~ 0.001 eV/Å⁻¹). The calculations of phonons is performed sampling the first Brillouin Zone with a $45 \times 45 \times 1$ k-grid (for the wavefunctions) and a $15 \times 15 \times 1$ q-grid (for the force constants). The formation of CDWs is analysed sampling the first Brillouin Zone by means of the following grids of **k**-points for the following supercells: $30 \times 30 \times 1$, $23 \times 23 \times 1$, $20 \times 20 \times 1$, $17 \times 17 \times 1$, and $15 \times 15 \times 1$ for the 2×1 , $\sqrt{7} \times \sqrt{7} \times 1$, $3 \times 3 \times 1$, $\sqrt{13} \times \sqrt{13} \times 1$, and $4 \times 4 \times 1$ supercells, respectively, keeping approximately an equal distance between **k**-points.

II. RESULTS

We undertake an investigation of many possible modulations via a unit-cell phonon study combined with total energy calculation, and compare our results to recent findings, showing a considerable agreement between the observed stripe character and the 4×4 modulation [S3, S4]. It is worth noting that our results are obtained for isotropic in-plane, instead of uniaxial strain [S5].

Despite phononic signatures for a $\sqrt{7} \times \sqrt{7}$ reconstruction are weak (the instabilities run into that direction, but they are still far from it), supercell calculations have been performed in such supercell; no stable CDW has been found - i.e., among all the distortions tested, all of them relaxed, with the same energy, to the undistorted structure.

The structures in the $\sqrt{13} \times \sqrt{13}$ periodicity retain some structural features of the HX, CC, and HC structures of the 3×3 periodicity, and are named, accordingly, chalcogen centered triangle with threefold counterclockwise star (CCccws), hexagonal with small chalcogen centered triangle (HXCC), and hollow centered large triangle (HC), see TABLE I in main text and FIG. S3.

Addressing the question on the complex coexistence of CC and HC phases [S6], we advance the hypothesis that it occurs along boundaries of a 2×3 CDW. Energy comparison with the other CDW structures - TABLE I in the main text- puts it on solid grounds. Eventually, we argue that an incipient stripe character is present even in the 3×3 periodic structures, which coexist with their related higher symmetric phases, in agreement with recently predicted doping-driven structures [S7].

We also show the charge distribution of the 4×4 $3\mathbf{q}$ phase computed for different energy intervals in FIG. S6. The charge distribution visualized at different energies shows different peaks and troughs. The displacement of the maxima with respect to the underlying structure is referred to as CDW phase, and its change is related to the emergence of a CDW energy gap [S8]. The case of the $3\mathbf{q}$ CDW is quite interesting because its DOS shows a dip around -0.08 eV. However, it is farther from Fermi level that its phase shows remarkable changes.

In the STM studies used for comparison, the coexistence of different modulations and CDW structures is likely due to local strain. Regions with different different interlayer coupling (between the NbSe₂ layer and the substrate), may correspond to different values of strain, governing the $3\mathbf{q}$ and $1\mathbf{q}$ regions separation. In addition, coexistence of different modulation and/or CDW structures may result from a complex energy hierarchy between modulations and between structures, where in-plane strain may play a role in changing such hierarchy.

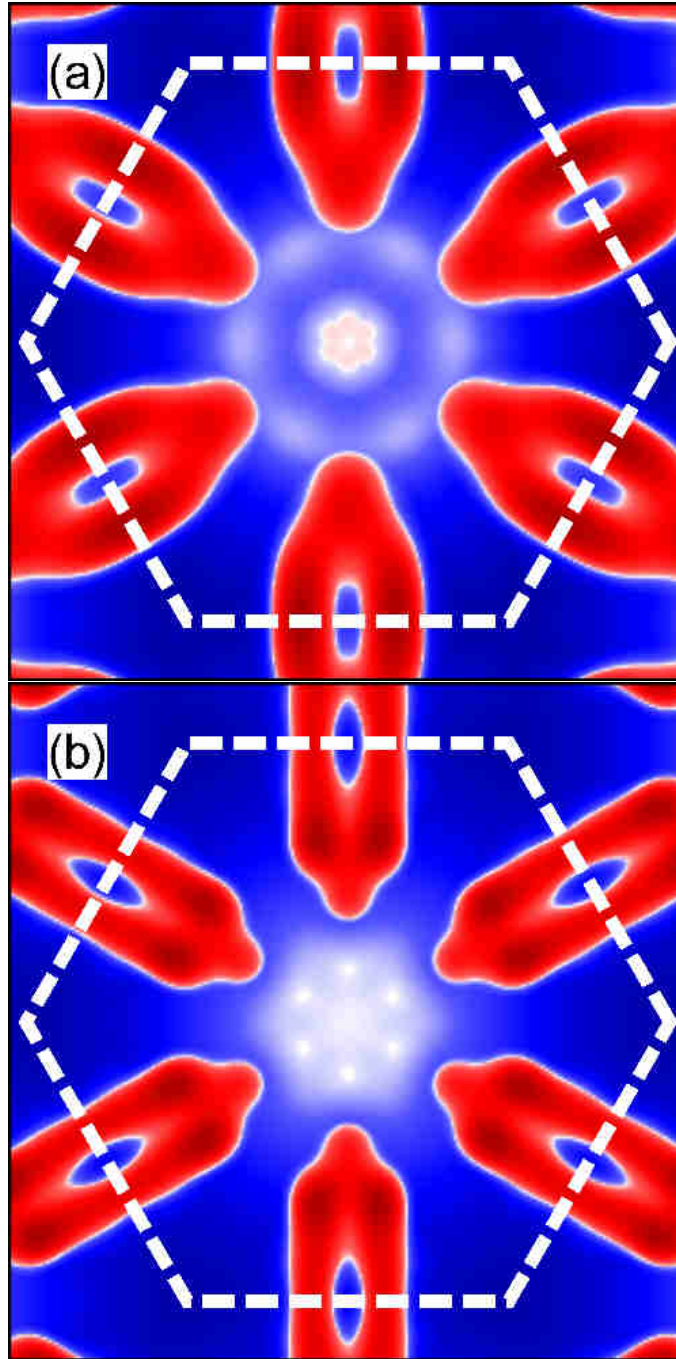


FIG. S1. Phonon dispersion for the single layer and bulk without van der Waals corrections. It is evident how the bulk does not feature phonon instabilities away from the Γ M line, apart from those surrounding the M point.

-
- [S1] J. P. Perdew, K. Burke, and M. Ernzerhof, *Phys. Rev. Lett.* **77**, 3865 (1996).
[S2] J. P. Perdew, K. Burke, and M. Ernzerhof, *Phys. Rev. Lett.* **78**, 1396 (1997).
[S3] A. Soumyanarayanan, M. M. Yee, Y. He, J. van Wezel,

- D. J. Rahn, K. Rossnagel, E. W. Hudson, M. R. Norman, and J. E. Hoffman, *Proc. Natl. Acad. Sci.* **110**, 1623 (2013).
[S4] S. Gao, F. Flicker, R. Sankar, H. Zhao, Z. Ren, B. Rachmilowitz, S. Balachandar, F. Chou, K. S. Burch,

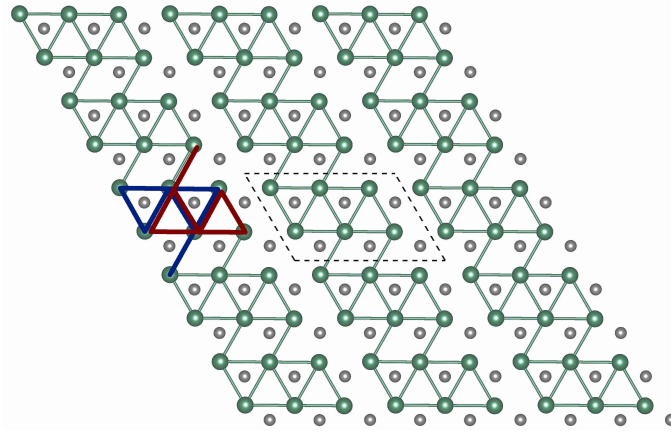


FIG. S2. Structure of the relaxed 2×3 CDW resulting in a stripe phase. Along with the CDW structure, the representative CC and HC CDW structures from the 3×3 periodicity are traced in red and blue, respectively, in order to show how they merge in the 2×3 cell. The dashed lines mark the supercell used for the simulation.

- Z. Wang, J. van Wezel, and I. Zeljkovic, *Proc. Natl. Acad. Sci.* **115**, 6986 (2018).
- [S5] F. Flicker and J. van Wezel, *Phys. Rev. B* **92**, 201103 (2015).
- [S6] G. Gye, E. Oh, and H. W. Yeom, *Phys. Rev. Lett.* **122**, 016403 (2019).
- [S7] F. Cossu, A. G. Moghaddam, K. Kim, H. A. Tahini, I. Di Marco, H.-W. Yeom, and A. Akbari, *Phys. Rev. B* **98**, 195419 (2018).
- [S8] C. J. Arguello, S. P. Chockalingam, E. P. Rosenthal, L. Zhao, C. Gutiérrez, J. H. Kang, W. C. Chung, R. M. Fernandes, S. Jia, A. J. Millis, R. J. Cava, and A. N. Pasupathy, *Phys. Rev. B* **89**, 235115 (2014).

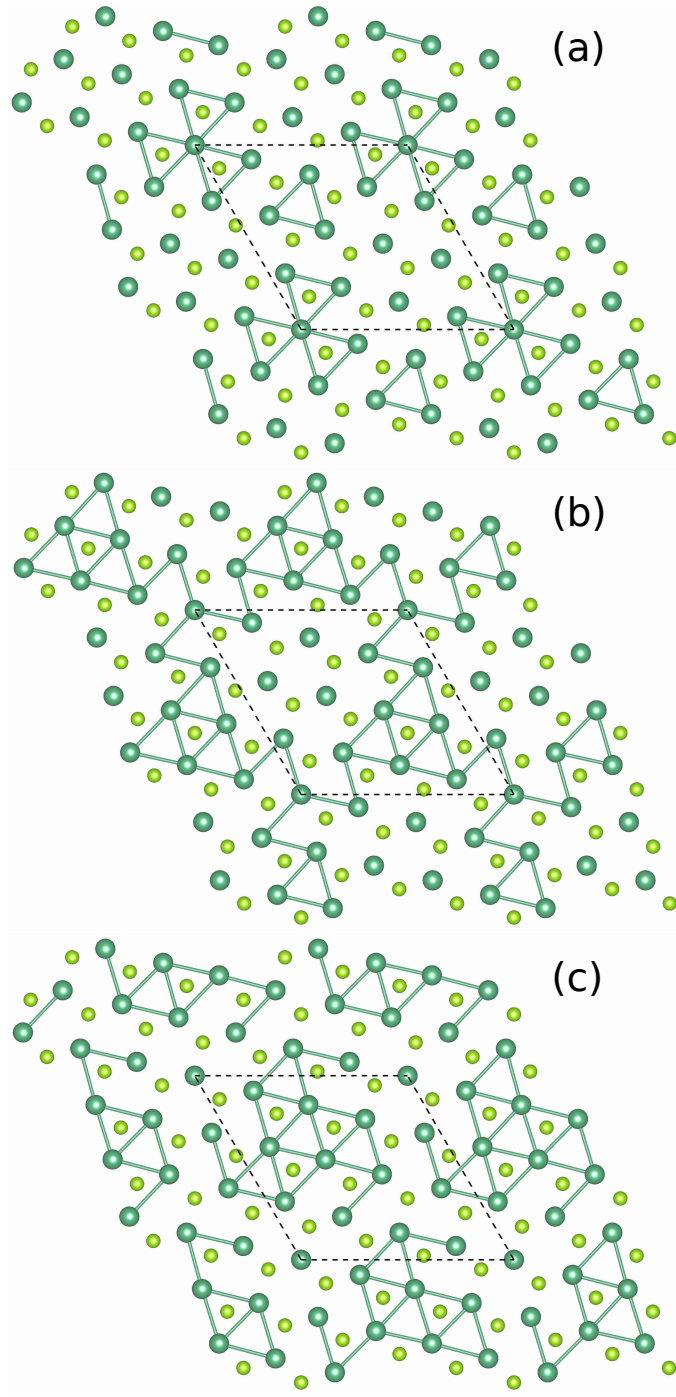


FIG. S3. Structure of the relaxed $\sqrt{13} \times \sqrt{13}$ CDW resulting in a stripe phase. The CDW structures resemble those with the 3×3 periodicity, HX, CC, and HC; in the present case, these structures are the CCcws (a), the HXCC (b), and the HC (c) - see text for more details. The dashed lines mark the supercell used for the simulation.

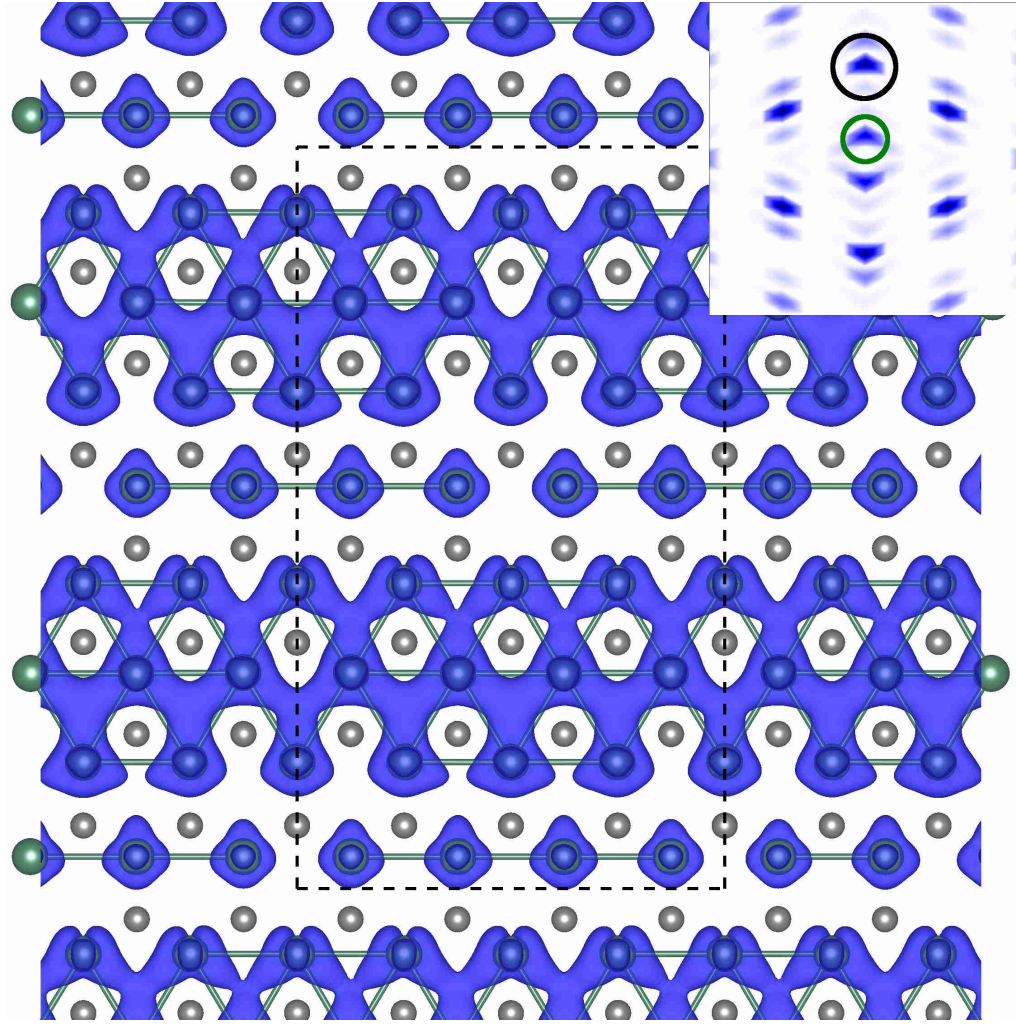


FIG. S4. This figures show the structure of the 4×4 periodicity under compressive strain (however, note that the strain slightly affects the charge distribution); the modulation has a wavelength of $\sim 14\text{\AA}$, as shown also in the main text. Inset: FT of the charge distribution, where the black circle marks one of the Bragg peaks and the green circle marks one of the 4×4 CDW peaks.

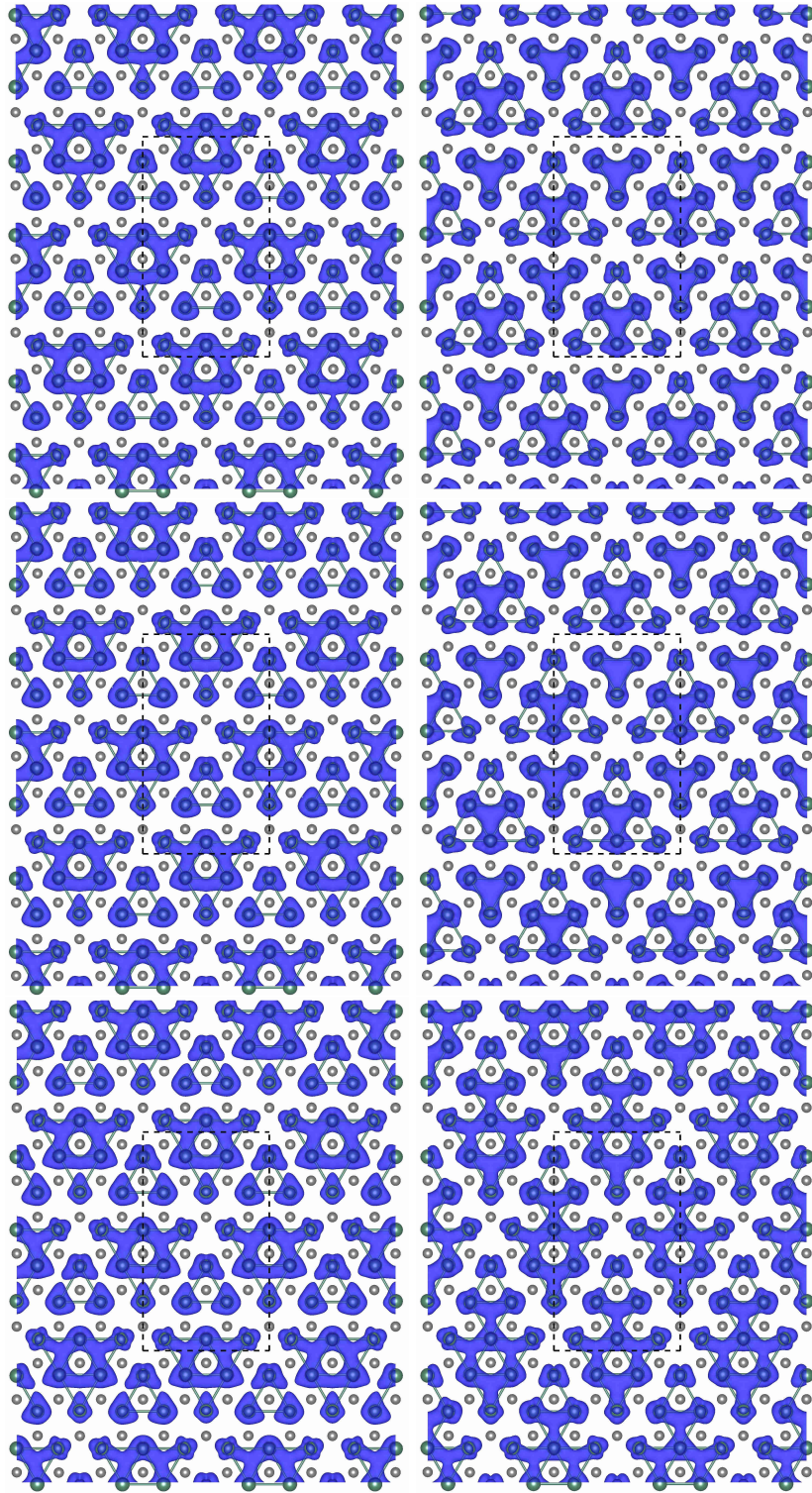


FIG. S5. This figures show how the HC and the CC CDW structures and charge distributions become similar under compressive strain.

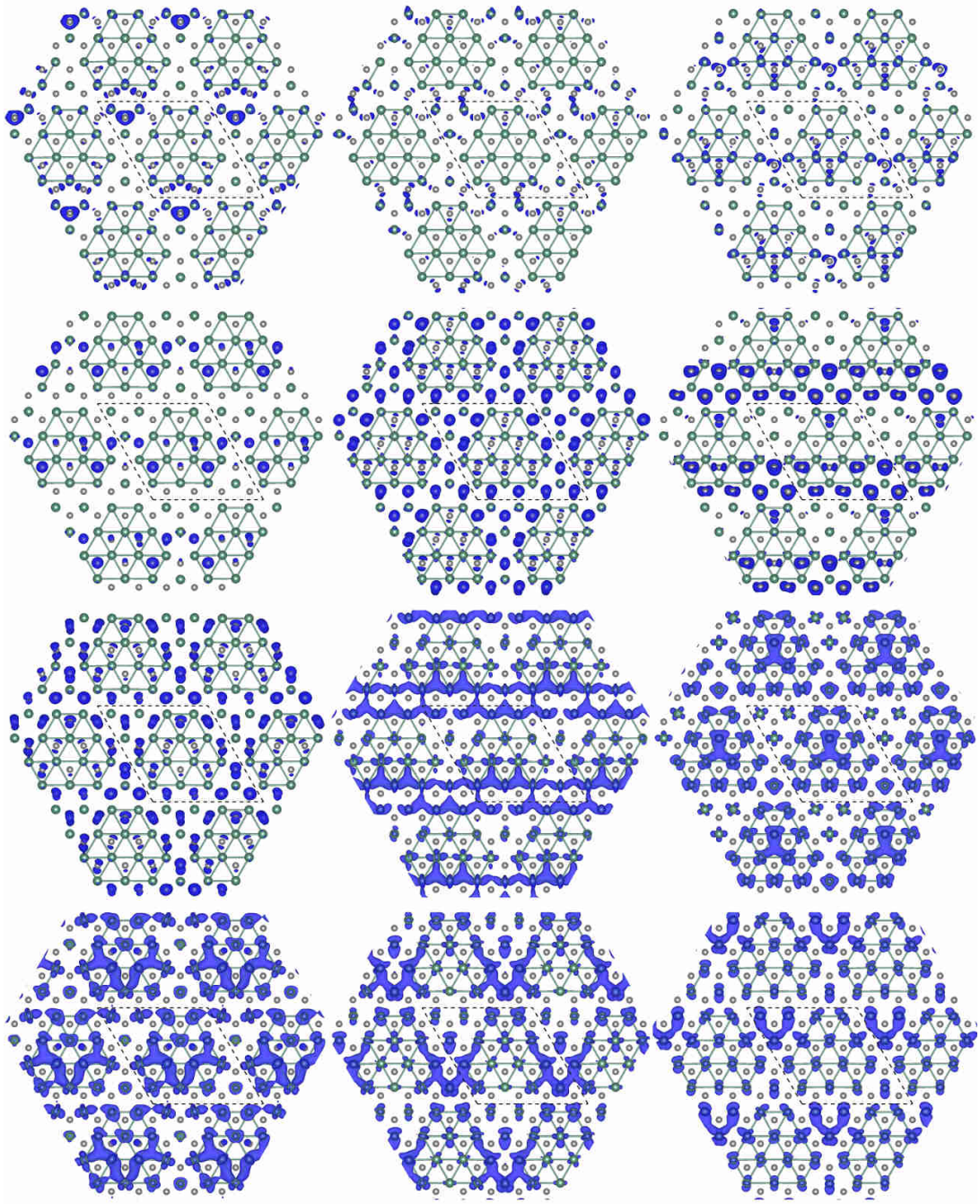


FIG. S6. Charge distribution of the $3\mathbf{q}$ CDW integrated at different energy ranges (corresponding to simulated dI/dV maps at different biases).

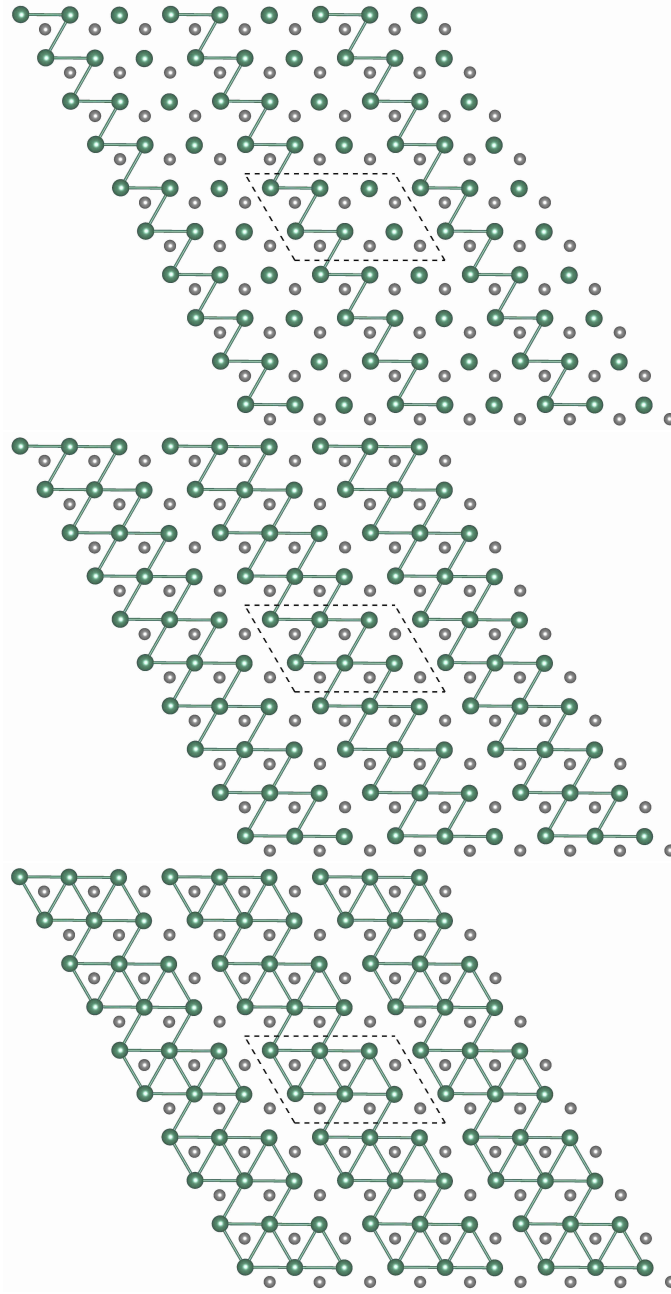


FIG. S7. These figures are intended to highlight how the Nb-Nb bonds pattern of the 2×3 appears; left, centre, right highlight the bonds with 98%, 99%, and 100% of the lattice constant, respectively. Note its stripe character, and the mixing of HC and CC CDWs, as they merge along the \mathbf{a}_2 lattice vector, see also FIG. S2.